Tidal effects and periastron events in binary stars

Gloria Koenigsberger & Edmundo Moreno
Universidad Nacional Autónoma de México
gloria@fis.unam.mx; edmundo@astroscu.unam.mx

December 8, 2008

ABSTRACT

Binary stars in eccentric orbits are frequently reported to present increasing levels of activity around periastron passage. In this paper[1] we present results of a calculation from first principles of the velocity field on the surface of a star that is perturbed by a binary companion. This allows us to follow the orbital phase-dependence of the amount of kinetic energy that may be dissipated through the viscous shear, $\dot{E}$, driven by tidal interactions. For stars with relatively small stellar radii compared with the orbital separation at periastron ($R_1/r_{per} \leq 0.14$), a clear maximum occurs before periastron passage for sub-synchronous rotation and after periastron for super-synchronous rotation. For larger stellar radii however, $\dot{E}$ oscillates over the orbital cycle and periastron passage does not cause a particularly greater enhancement in energy dissipation rates than some of the other orbital phases. Finally, we perform exploratory calculations for a

[1]Based on the poster presented at *Hot Massive Stars...A lifetime of Influence*, Workshop held at Lowell Observatory, 2008 October 12–15, celebrating Peter Conti's birthday

WR/LBV binary system that in 1993-1994 underwent an LBV-like eruption, HD 5980. Our $\dot{E}$ calculations reproduce the oscillations that appear around periastron passage in HD5980's recent visual light curve. We suggest that the energy dissipation from tidal flows in asynchronously rotating binary stars may provide a mechanism by which evolving stars may be driven into an active state. Given the nature of the tidal perturbations, the resulting mass-loss distribution is expected to be non-uniform over the stellar surface and highly time-dependent.

1 Introduction

A number of binary systems show evidence of enhanced activity around periastron passage. Among these, η Car is the most extreme and best documented example of periodic brightening at X-ray, visual and IR wavebands associated with periastron passages. Recently, van Genderen & Sterken[2] suggested that these periastron events may have the same physical cause as the milder "periastron effects" exhibited by many less renowned eccentric binaries in which small enhancement ($\Delta \mathrm{m}_v$ $\sim$0.01–0.03^{mag}) in the visual brightness of the system around periastron passage are observed. They suggested that the fundamental cause of the effects may reside in the enhanced tidal force present during periastron passage.

Our study of tidal interactions and their potential role in sparking stellar activity was first inspired by the peculiar behavior of the WR/LBV system HD 5980.[3] In particular, the orbital phase-dependent behavior of the line-profile variations led us to raise the question of whether the periastron passage

[2]2007, IBVS, 5782

[3]Koenigsberger, G. 2004, RMAA,40, 107; Georgiev, Hillier & Koenigsberger, this meeting.

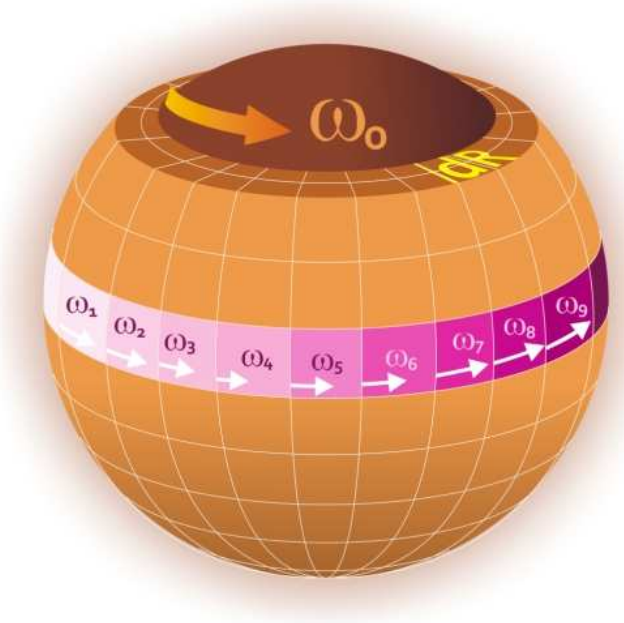

Figure 1: Artistic representation of the one-layer model for the tidal interaction calculations. The inner body of the star is assumed to rotate uniformly, while the perturbations acting on the surface layer produce a velocity field leading to local angular velocities that differ from the underlying uniform rotation.

could affect the intrinsic stellar wind properties, possibly enhancing the mass-loss rate around this phase.[4]. Our objective is to explore whether the mechanism involved in causing the instabilities is the dissipation of kinetic energy of the viscous flows that are driven by the tidal interactions.

2 Method for $\dot{E}$ calculation

A system is in synchronous rotation when the orbital angular velocity Ω equals the angular velocity of rotation ω_0. In eccentric orbits, the degree of synchronicity varies with orbital phase. We use periastron passage as the reference point for defining the synchronicity parameter $\beta_{per} = \omega_0/\Omega_{per} = 0.02P\frac{v_{rot}(1-e)^{3/2}}{R_1(1+e)^{1/2}}$, where e is the orbital eccentricity, the rotation velocity v_{rot} is

[4]Koenigsberger et al. 2002, ASPCS 260, 507

given in km/s, the orbital period P is given in days, and the stellar equilibrium radius R_1 is given in solar units. When at any orbital phase $\beta \neq 1$, non-radial oscillations are excited, driven by the tidal interactions. We refer to the azimuthal component of the forced oscillations as "tidal flows".

Our method consists of computing the motion of a Lagrangian grid of surface elements distributed along a series of parallels (i.e., rings with different polar angles) covering the surface of the star with mass M_1 as it is perturbed by its companion of mass M_2. The main stellar body below the perturbed layer is assumed to have uniform rotation. The equations of motion that are solved for the set of surface elements include the gravitational fields of M_1 and M_2, the Coriolis force, and gas pressure. The motions of all surface elements are coupled through the viscous stresses included in the equations of motion. The kinetic energy of the tides may be dissipated through viscous shear, thus leading to an energy dissipation rate, $\dot{E}$. The rate of energy dissipation per unit volume is given by the matrix product $\dot{E} = -\mathbf{P}_\eta : \nabla \boldsymbol{v}$, where $\mathbf{P}_\eta$ is the viscous part of the stress tensor and $\boldsymbol{v}$ is the velocity of a volume element with respect to the center of the star.[5].

The benefits of our model are: 1) we make no *a priori* assumption regarding the mathematical formulation of the tidal flow structure since we derive the velocity field $\boldsymbol{v}$ from first principles; 2) the method is not limited to slow stellar rotation rates nor to small orbital eccentricities; and 3) it is computationally inexpensive.

[5]For details see Moreno & Koenigsberger 1999, RMAA, 35, 157; Moreno et al. 2005, A&A, 437, 641; and Toledano et al. 2007, A&A, 458, 413

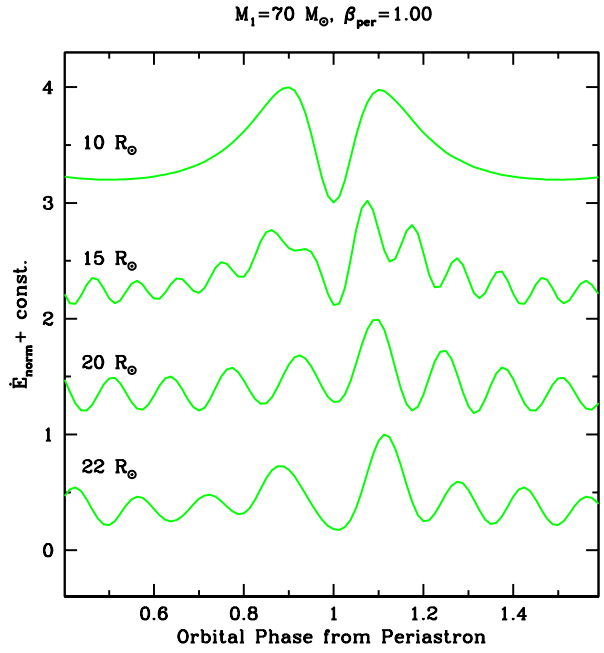

Figure 2: Energy dissipation rates plotted as a function of orbital phase for a M_1 =70 $M_\odot$ primary star of different stellar radii. In all cases, the star is in synchronous rotation at periastron (ϕ =1). $\dot{E}$ is normalized to its maximum value over the orbital cycle. P=19.3d and e=0.3.

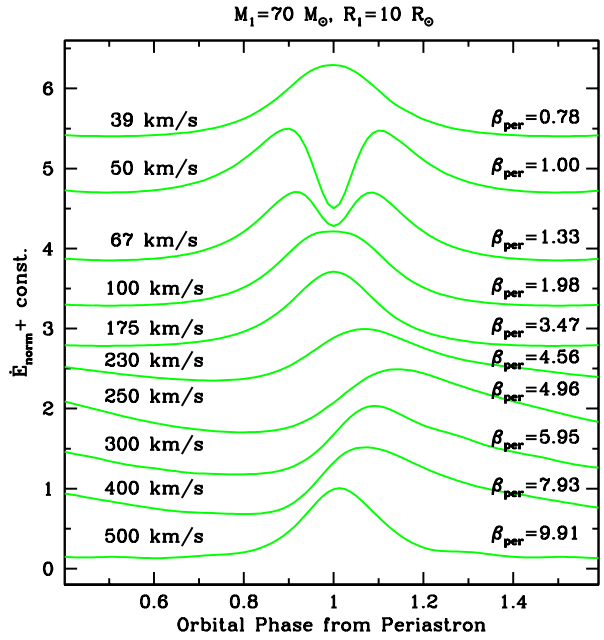

Figure 3: $\dot{E}$ plotted as a function of orbital phase for a 70 $M_\odot$, R_1 =10 $R_\odot$ binary system with stellar rotation velocities 19–438 km/s. Maximum $\dot{E}$ values always occur within $\pm$0.1 in phase from periastron.

3 Dependence on stellar radius and rotation velocity

For simplicity, we first consider a primary star that is synchronously rotating at periastron; i.e., β_{per} =1. Figure 2 illustrates the behavior of energy dissipation rates as a function of orbital phase for a 70+54 $M_\odot$ binary system with P =19.3 d, e =0.3 and values of R_1 =10–22 $R_\odot$. For small radii, the equilibrium tide component dominates. Thus, the trend for increasing $\dot{E}$ as periastron is approached reverses just before periastron, and goes to minimum at this phase since this is when β_{per} =1. For stars with larger radii, however, the dynamical tide dominates, and $\dot{E}$ presents an oscillatory behavior over the orbital cycle.

Figure 3 illustrates the result of holding constant R_1 =10$R_\odot$ and varying v_{rot} from sub-synchronous to highly super-synchronous values. The maximum $\dot{E}$ occurs close to periastron passage, but not necessarily centered at this orbital phase. We refer to the maximum value attained by $\dot{E}$ over the orbital cycle as $\dot{E}_{Max}$.

Figures 4–6 summarize the behavior of $\dot{E}_{Max}$ as a function of stellar radius and of rotation velocity for the set of models listed in the Table, and Figure 7 plots the phase when this maximum is attained. $\dot{E}_{Max}$ occurs before periastron passage in sub-synchronous starsr and after periastron when stars rotate super-synchronously.

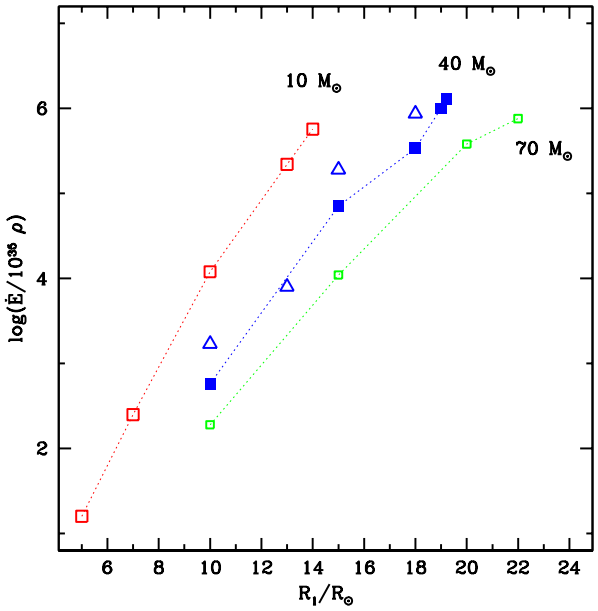

Figure 4: $\dot{E}_{Max}$ plotted as a function of stellar radius for the β_{per} =1 calculations listed in the Table. ρ is the mean density of the layer where the energy is dissipated. Squares correspond to cases with P=19.3, e=0.3 and triangles to P =100 d, e =0.767.

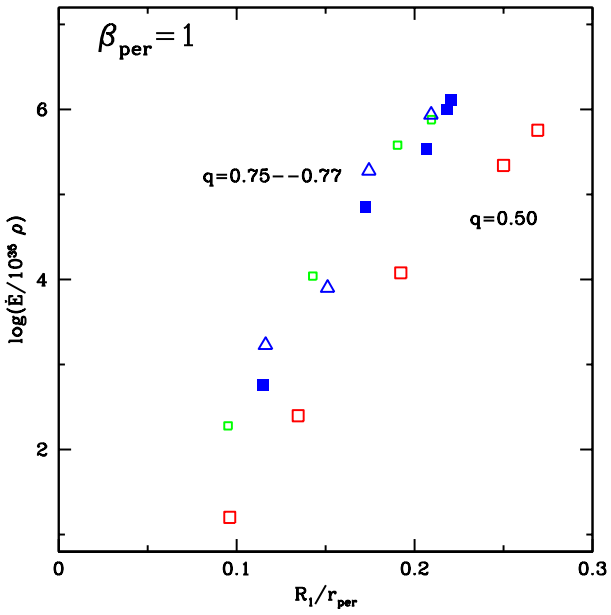

Figure 5: Same as previous figure, but here the abscissa is given in units of stellar radius normalized to the orbital separation at periastron. The mass-ratio, q =M_2/M_1 is listed. Colors are as in Fig. 4.

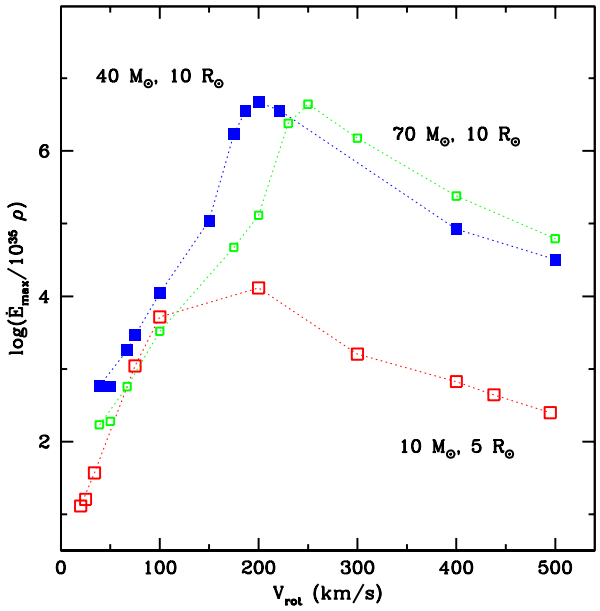

Figure 6: $\dot{E}_{Max}$ for the binary system models with P=19.3 d and e=0.3 plotted as a function of equatorial rotation velocities. Note that ever-increasing rotation velocity does not produce an ever-increasing $\dot{E}_{Max}$.

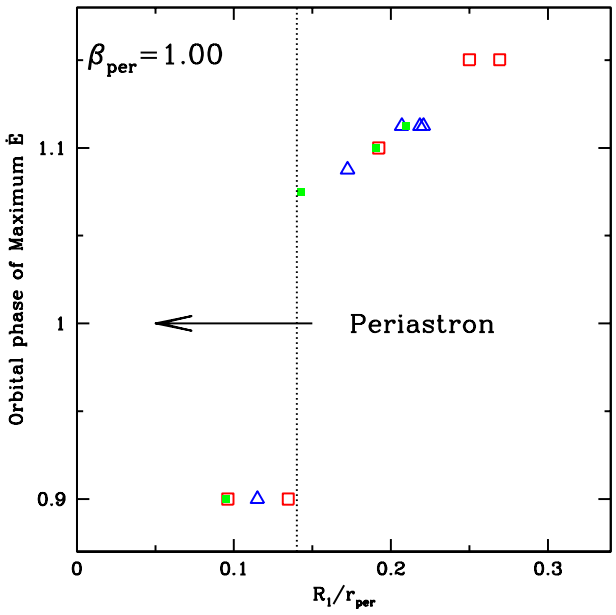

Figure 7: Orbital phase when $\dot{E}_{Max}$ occurs for the β_{per} =1 cases for M_1 = 10 $M_\odot$ (red); 40 $M_\odot$ (blue); 70 $M_\odot$ (green). The dotted line shows that for stars with $R_1/r_{per} \leq 0.14$, $\dot{E}_{Max}$ occurs before periastron passage while for stars with larger relative radii, it occurs after periastron.

Table 1: Summary of binary system models

M_1 ($M_\odot$)	M_2 ($M_\odot$)	P (days)	e	r_{per} ($R_\odot$)	R_1 ($R_\odot$)	V_{rot} (km/s)	β_0	$< \dot{E}_{max}/\rho >$ (10^{35}ergs-cm^3/s-g)
10	5	19.3	0.30	52	5–14	25–71	1.000	0.16×10^2–0.57×10^6
40	30	19.3	0.00	74	10	50	1.000	0.10×10^{-2}
40	30	19.3	0.30	87	10–19.2	50–97	1.000	0.58×10^3–0.13×10^7
40	30	100.0	0.767	86	10–18	59–107	1.000	0.17×10^4–0.87×10^6
40	30	100.0	0.31	256	13	13	1.000	0.10×10^1
70	54	19.3	0.30	105	10–22	50–111	1.000	0.19×10^3–0.76×10^6
10	5	19.3	0.30	52	5	20–495	0.79–19.63	0.13×10^2–0.25×10^3
40	30	19.3	0.30	87	10	39–500	0.78–2.97	0.59×10^3–0.47×10^7
40	30	100.0	0.767	86	10	39–500	0.65–5.08	0.28×10^4–0.44×10^7

4 Periastron effect in HD 5980 ?

Figure 8 is a comparison of the recent visual light curve of HD 5980[6] (kindly provided by P. Massey) with the $\dot{E}$ values obtained from our model calculation for a 70+54 $M_\odot$ binary with β_{per} =1.33 and R_1 =21 $R_\odot$. The model qualitatively reproduces the behavior after periastron, suggesting that the tidal flows mechanism may be playing an important role in this system. Particularly interesting also is the apparent increase in the overall energy flux emitted around periastron (ϕ =0.15) in the wavelength range $\lambda\lambda$1000–10000 Å. Illustrated in Figure 9 is the ratio of the spectral energy distribution from HST/STIS observations of 1999 and FUSE observations of 2002. This indicates that either there is a significant redistribution in the SED around periastron and/or there is an added source of energy. Hence, HD 5980 appears to belong in the list of binaries that present a periastron effect. Furthermore, we speculate that tidal flows may also provide a mechanism to explain the occasional

[6]Foellmi et al. 2008, RMAA, 44,3

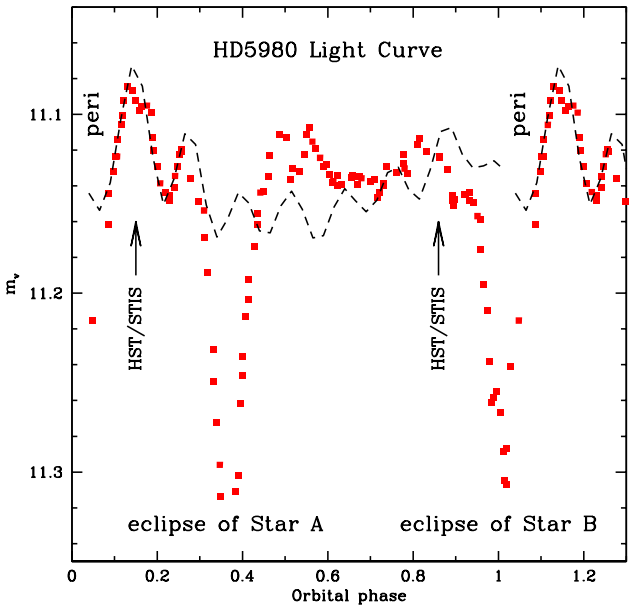

Figure 8: V-magnitude light curve of HD 5980 (from P. Massey) compared with the tidal energy dissipation curve assuming R_A =21 $R_\odot$ and β_0 =1.33. Times of eclipses and periastron passage are indicated, as well as phases when the 1999 HST/STIS spectra were obtained.

luminous blue variable-like eruptive behavior.

We suggest the following working scenario: If the erupting star in HD 5980 is in the process of leaving the Main Sequence[7], its systematically increasing radius should lead to values of $\dot{E}$ that grow exponentially, as shown in Figs. 4 and 5. At some point, a critical radius could be reached at which the sum of $\dot{E}$ and the intrinsic luminosity of the star becomes super-Eddington, thus producing an episode of strongly enhanced mass-loss, which we would observe as an eruptive event. The frequency of this type of episodes might be expected to depend on the expansion rate of the star, the depth of the layer in which most of the energy dissipation takes place and the amount of mass that is ejected each time the critical radius is attained.

[7]as implied by its He/H abundance, Koenigsberger et al. 1998, ApJ, 499, 889.

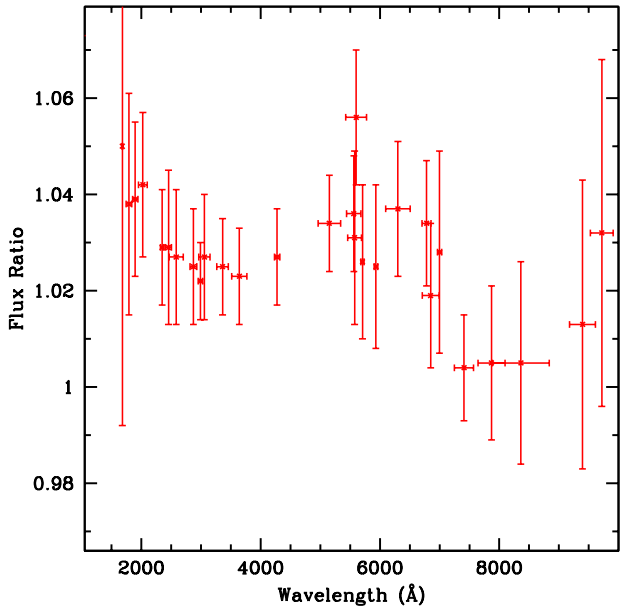

Figure 9: Ratio of HST/STIS spectra observed at orbital phases 0.15 and 0.83 in 1999. Error bars are rms of mean for wavelength range indicated by error bars for abscissa.

5 Discussion and future directions

The periastron events of η Carinae, WR 140 and WR 125 are generally modeled in the context of interacting winds theory.[8] These models have been mostly successful, although some discrepancies remain.[9] It is interesting to note that one of the discrepancies involves the time of maximum X-ray emission, which does not always appear at periastron passage as predicted by the wind-wind collision models. An explanation for this discrepancy may reside in that the mass-loss rate and wind velocity structure of the stars does not remain constant over the orbital cycle. As shown above, the tidal flows model predicts a significant perturbation of the stellar surface which, in turn, could significantly

[8]see Parkin & Pittard, 2008, MNRAS, 388,104, and references therein.
[9]see, for example, Rauw, G., 2008, RMAACS, 33, 59.

affect the stellar wind properties of the stars.

A further consequence of the tidal flows model is that the strongest perturbation should occur on the larger of the two stars in the binary system. In the case of the WR+O binary systems, the O-star companion generally has the larger stellar radius. Hence, in a system such as WR 140 it is conceivable that periastron passage could lead to a significant increase in the *O-star's* wind momentum. Assuming this to be the case, the possibility then exists that the O-star's wind could dominate the momentum ratio around periastron, thus even inverting the orientation of the shock cone geometry.

Finally, it is interesting to note that the action of tidal flows is not distributed symmetrically over the stellar surface and thus, if the energy dissipated by these motions contributes towards mass-loss, the additional outflow is expected to depart from spherical symmetry as well. Furthermore, the critical radius could be reached by the star several times during its late stages of evolution, thereby producing multiple episodes of enhanced mass-loss prior to its demise in the supernova event. An interesting problem would be to analyze the morphology of circumstellar structures that may be produced from such asymmetric mass-ejections as well as the manner in which this distribution of matter then may affect the expansion of the supernova ejecta.

In conclusion, the tidal flows produced in asynchronously rotating binary systems provide a mechanism that may explain a wide variety of observational phenomena ranging from periodic photospheric line-profile variability to episodic and asymmetric mass-shedding events. The actual magnitude of the energy dissipation rates depends strongly on the viscosity parameter that is assumed for the stellar material and on the depth of the layer

where the energy dissipation rates are most significant. A proper assessment of these physical parameters will help determine the actual importance of the role being played by asynchronous rotation and tidal flows in producing peculiar phenomena observed in binary stars.

6 Acknowledgements

This research was supported by UNAM/DGAPA through PAPIIT grants IN 119205 and IN 106708, and CONACYT.